Iranian Journal of Catalysis 6(5), 2016, 447-454

IRANIAN JOURNAL OF CATALYSIS

Photocatalytic oxidation of an organophosphorus simulant of chemical warfare agent by modified TiO_2 nanophotocatalysts

Abbas Besharati-Seidani*

Department of chemistry, Malek Ashtar University of Technology, Tehran, Iran.

Received 20 September 2015; received in revised form 13 August 2016; accepted 21 August 2016

ABSTRACT

TiO_2 nanoparticles, as a photocatalyst for oxidation of dimethyl methylphosphonate (DMMP) as an organophosphorus simulant of chemical warfare agent, were prepared by using sol-gel method. The prepared nanoparticles were then modified with transition metals in order to decrease the electron-hole recombination and increase the photocatalytic activity. Transition metal ions including Pt, Pd and Ni were used for this purpose. The prepared samples were characterized by different analysis methods, and Photocatalytic mechanism was studied over the unmodified and modified photocatalysts. The effect of some operational parameters such as catalyst dosage, initial DMMP concentration and type and amount of loading the transition metal on the photocatalytic activity was investigated. The results showed that the best photooxidation of DMMP was obtained with 1% Pd/TiO_2. The optimum conditions for catalyst dosage and initial DMMP concentration were 20 g L^{-1} Pd and 0.138 M, respectively.

***Keywords**: DMMP, Nanoparticles, Photooxidation, TiO_2, Transition metals.*

1. Introduction

Nowadays, there is a great problem for water purification from different pollutants. Many pollutants like insecticides, pesticides and detergents are organophosphorus compounds. These pollutants are commonly resistant against oxidation because they are generally stable to heat, light and oxidizing agents [1,2]. The pollutants presence in water would be a harmful factor for aquatic life. Photocatalytic oxidation is a very interesting and promising method for degradation of pollutant compounds in the aqueous mediums [3]. Synthesis, characterization and investigation of photocatalytic activity of some photocatalysts were reported by authors in the literature [4-7]. Photocatalytic oxidation of some organophosphorus pesticides (acrinathrin, methamidophos, malathion, diazinon, carbetamide) and insecticide fenitrothion was reported previously [8-11]. Most of these materials are carcinogenic and mutagenic and their degradation is great of importance because of the difficulties in treating them by conventional methods.

*Corresponding author email: abbasbesharati@yahoo.com
Tel: +98 21 2297 0224; Fax: +98 21 2297 0224

There are a variety of techniques such as coagulation, adsorption, advanced oxidation with ozone (O_3), hydrogen peroxide (H_2O_2) and ultraviolet (UV) for effectively treating dangerous compounds in the aqueous environments. UV oxidation is a destruction process that oxidizes organic and explosive constituents in water by the addition of strong oxidizers and irradiation [12-17]. Oxidation of target contaminants is caused by direct reaction with the oxidizers, UV photolysis, and through the synergistic action of UV light. If complete mineralization is achieved, the final products of oxidation will be carbon dioxide, solvent, and salts. UV oxidation processes can be configured in batch or continuous flow modes, depending on the throughput under consideration [18-22]. Advanced oxidation processes (AOPs), are based on generation of very reactive species such as Hydroxyl radical ($OH^{\bullet}$) and Superoxide anion radical ($O_2^{-\bullet}$). These radicals are generated when a semiconductor catalyst absorbs radiation in solution [23-27]. Using heterogeneous photocatalysis is one of the most promising approaches in this regard. This technique is based on the photoexcitation of a semiconductor photocatalyst with the adsorption of photons energy equal to or greater than the band gap.

Titanium dioxide (TiO_2) is used as photocatalyst because of its optical and electronic properties, low cost, chemical stability and non-toxicity [28,29]. Its photocatalytic activity depends on the crystalline phase, particle size and morphology. The band gap energy of anatase TiO_2 and rutile TiO_2 are 3.23 eV and 3.02 eV, respectively. Anatase shows the higher photocatalytic activity. However, anatase TiO_2 has the disadvantages such as low specific surface area, poor thermal stability, poor mechanical strength and lack of abrasion resistance [26-28]. TiO_2 utilizes only a very small fraction of the solar spectrum. Its coupling with a small band gap semiconductors or doping with transition metal ions extends light absorption into the visible region [29].

An important group of environmental contaminations in the war conditions are caused by chemical warfare agents (CWAs) including blister agents such as distilled mustard and lewisite, and nerve agents such as tabun, sarin, and soman. These agents can also contaminate the aqueous environments. Thus, purification of the water environments from these pollutants is of interest to researchers. Because CWAs are highly toxic and their use is restricted in nonsurety laboratories, research on the environmental fate of CWAs is often conducted using simulant compounds. An ideal chemical agent simulant would mimic all relevant chemical and physical properties of the agent without its associated toxicological properties. Thus, a number of different chemicals have been used as CWA simulants depending on the physical–chemical property of interest. DMMP was used as a nerve agent simulant in the environmental fate of nerve agents [30] and has organophosphorus structure.

In this work, after production of the unmodified and modified nanophotocatalysts and investigation of their properties according to our pervious published paper [31], photocatalytic behavior of them in the photooxidation of DMMP as a nerve agent simulant was examined through some experiments. Finally, the effect of some parameters such as catalyst dosage, initial DMMP concentration and type and amount of loading the transition metal and photooxidation time of DMMP on the photocatalytic activity was investigated.

2. Experimental

2.1. Materials

Tetraisopropyl orthotitanate, ethanol, ethanolamine, $Ni(NO_3)_2$, $Pd(CH_3COO)_2$ and $H_2PtCl_6.6H_2O$ were obtained from Merck. Dimethyl methylphosphonate was purchased from Sigma Aldrich. All materials were used without further purification.

2.2. Apparatus

X-Ray Diffraction (XRD) was used to identify crystalline phase with in instrument on a diffractometer (D_4 model) with Cu Kα radiation (λ=1.5406 Å). The crystalline size of the powder was obtained from XRD patterns by Scherrer equation. BET was used for determining specific surface area of the photocatalysts. DRS analysis was performed by using a CINTRA 40 instrument with Barium (II) sulfate. The morphology of samples was examined by using an instrument Philips XL30 SEM. The concentrations were monitored by GC (Agilent 6890). The oven temperature was programmed as follows: isothermal at 40°C for 3 min, from 40°C to 260°C at 10°C/min, and isothermal at 260°C for 1 min.

2.3. Preparation of TiO_2 nanoparticles

TiO_2 nanoparticles were prepared by dissolving 5 g tetraisopropyl orthotitanate in 10.72 g of ethanol and 5.36 g of Ethanolamine. The solution mixed and stirred for 2 h (solution 1). A mixture of 10.72 g ethanol and 0.32 g H_2O (solution 2) were added to solution 1. The obtained solution was stirred for 2 h until a gel was formed. The gel was aged 24 h at room temperature until the solvent was evaporated. It was then dried in oven at 105°C for 3 h and calcined at 300, 400, 450, 500, 600, 700, 800°C for 4 h. Then, TiO_2 nanoparticles were obtained [1].

2.4. Preparation of Ni, Pd and Pt-modified TiO_2 nanoparticles

Percentages of (0.5, 1 and 1.5 of Ni)/TiO_2 were prepared by dissolving corresponding amounts of nickel (II) nitrate in solution 2. This was then added to solution 1, and stirred for 2 h. The resulting product was dried at room temperature for one day and then calcined at 400, 450, 500°C for 4 h. Similar procedures were performed to prepare (0.5, 1 and 1.5% of Pd)/TiO_2 and (0.5, 1 and 1.5% of Pt)/TiO_2 by dissolving corresponding percentages of $Pd(CH_3COO)_2$ and $H_2PtCl_6.6H_2O$ respectively, in solution 2.

2.5. Catalytic activity test

The experiments were performed in Pyrex UV reactor with constant temperature equipped with an OSRAM 125 W high pressure mercury lamp source [32]. DMMP solutions with fixed concentration and photocatalyst dosage were poured into the reactor. The solution was stirred for 15 min at dark until solution became homogenous and the lamp was switched on. Remained concentrations of DMMP solution was measured after specific times by gas chromatography instrument.

3. Results and Discussion

3.1. Characterization of photocatalysts

The characterization of pure TiO_2 and modified TiO_2 nanoparticles (photocatalysts) was achieved by different analysis methods, such as XRD, SEM, BET, FTIR and DRS after their synthesis and calcination.

The modification of TiO_2 nanoparticles with transition metal ions Pt, Pd and Ni was achieved to decrease the electron-hole recombination by trapping the electrons. Adding a low percentage of metal ions can also improve the photocatalytic activity of photocatalysts. In order to examine this effect, addition of various amounts of Pt, Pd and Ni impurities was investigated.

3.1.1. XRD patterns

The XRD patterns of TiO_2 nanoparticles are shown in Fig. 1. As it is seen, the pattern at 300°C shows amorphous phase and do not show any crystalline phase. However, by increasing the calcination temperature to 400°C, anatase and rutile phase peaks grow. Increasing the calcination temperature caused an increase in amount of both phases. Also, the best ratio of anatase to rutile is observed at 500°C (Fig. 1). The crystalline size of TiO_2 nanoparticle was calculated from XRD patterns using scherrer equation at temperatures 400, 450, 500 and 700 °C and was 21.0, 32.0, 46.2 and 122.8 nm, respectively [1]. According to the scherrer equation, it is obvious that by increasing the temperature from 400 °C to 700 °C, the size of TiO_2 particles increases from 21.0 nm to 122.8 nm.

The XRD patterns of 0.5% Pt/TiO_2, 1% Ni/TiO_2 and 1.5% Pd/TiO_2 calcinated at 500°C are demonstrated in Fig. 2. Comparing the spectra with pure TiO_2 indicates that metallic Pt impurities has penetrated in the structure while there are no peaks for Pd and Ni.

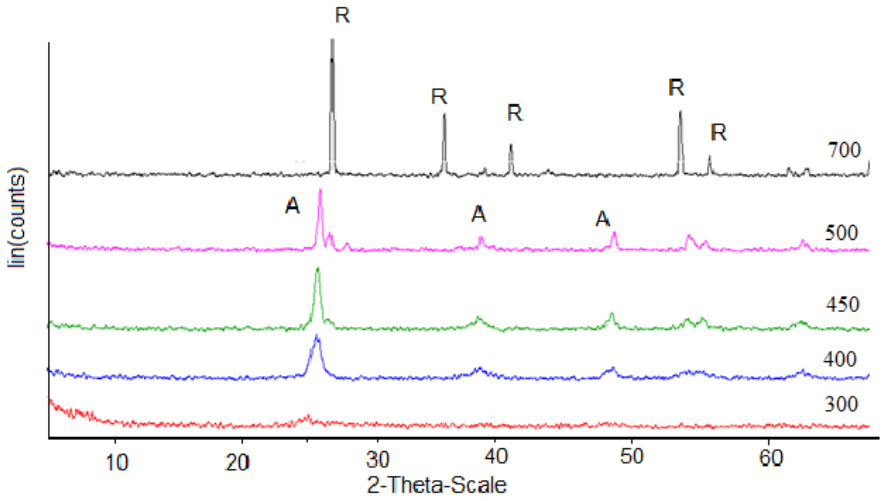

Fig. 1. XRD pattern of pure TiO_2 nanoparticles calcined at various temperatures.

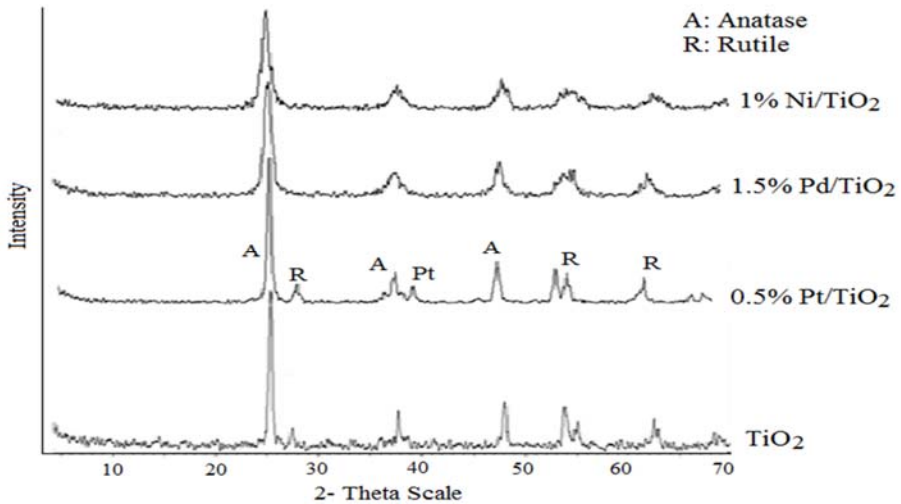

Fig. 2. XRD pattern of metal ion impregnated and bare TiO_2 photocatalysts calcinated at 500°C.

Therefore, it can be concluded that Pd and Ni are situated on surface of photocatalyst. Mean particle size of nanophotocatalysts was calculated from XRD patterns and was 37.5, 24.1 and 22.6 nm, respectively.

3.1.2. SEM analysis

Fig. 3 shows SEM micrographs of the prepared nanostructured 1% Ni/TiO_2, 1.5% Pd/TiO_2 and 0.5% Pt/TiO_2 photocatalysts that were calcinated at 500°C.

3.1.3. BET analysis

Table 1 and Table 2 give the results for BET surface area of pure TiO_2 nanoparticles calcinated at different temperatures and modified photocatalysts. It can be observed that increasing the temperature decreases the surface area. This happens because TiO_2 particles sinter at high temperature. Furthermore, the modification of TiO_2 by each transition metal causes the surface area to increase from the original value of 39.0 m^2 g^{-1} to 40.5 m^2 g^{-1} for 1% Ni/TiO_2**,** 44.8 m^2 g^{-1} for 0.5% Pt/TiO_2 and 64.4 m^2 g^{-1} for 1.5% Pd/TiO_2 (Table 2).

3.1.4. FT-IR spectroscopy

Fourier Transform Infrared (FT-IR) spectra of pure TiO_2 and modified TiO_2 were taken. A peak at 400-700 cm^{-1} in all samples is attributed to Ti-O stretching vibration, which shifts to lower wavelength by adding the transition metals. A progressive red shift in the band gap adsorption is noticed with metal loading. The adsorption is associated to the charge transfer from oxygen to titanium. The spectra of TiO_2 modified with Pt have the most red-shift in comparison with the others. Thus, it can be concluded that Pt is penetrated into the structure of TiO_2 more than Pd and Ni. The IR spectra of TiO_2 modified with transition metals don't show any bands corresponding to the other transition metal oxide, which is consistent with the XRD results.

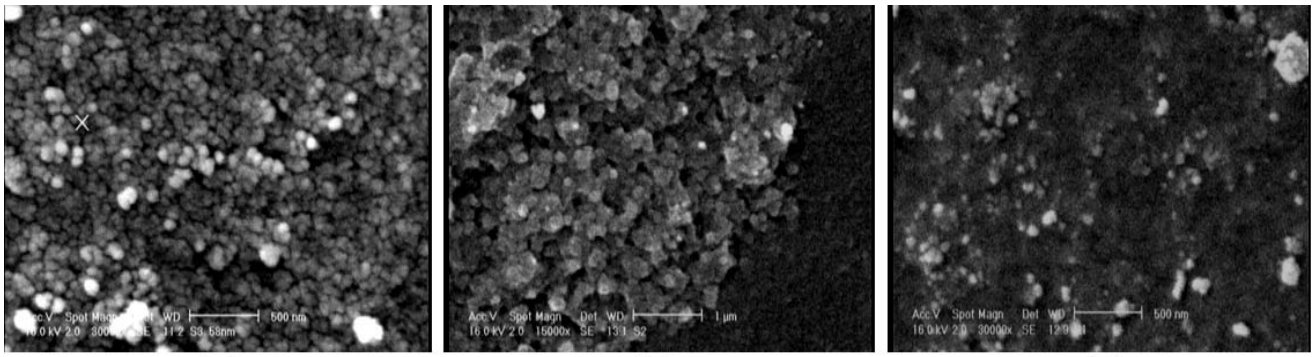

Fig. 3. SEM micrographs of: a) 0.5% Pt/TiO_2, b) 1.5% Pd/TiO_2 and c) 1% Ni/TiO_2 calcinated at 500 °C.

Table 1. BET surface area of TiO_2 nanoparticles at various calcination temperatures.

Calcination temperature (˚C)	Surface area (m^2 g^{-1})	Total pore volume (cm^3 g^{-1})
400	75.64	0.12
450	67.21	0.13
500	64.35	0.13

Table 2. BET surface area of metal doped TiO_2 nanoparticles.

Catalyst	Mean pore diameter (nm)	Surface area (m^2 g^{-1})	Total pore volume (cm^3 g^{-1})
TiO_2	10.20	39.0	0.90
1% Ni/TiO_2	84.90	40.5	0.08
0.5% Pt/TiO_2	80.14	44.8	0.16
1.5% Pd/TiO_2	94.70	64.4	0.13

3.1.5. DRS analysis

The band gap energy of the catalysts is determined using DRS (Diffuse Reflectance Spectra). A spectrophotometer equipped with an integrating sphere, and Barium Sulfate is used as a reference. The spectra are recorded at room temperature for 350<λ<800 nm. The energy band gaps of catalysts are calculated according to the Eq. (1).

$$E_g = hc/\lambda \quad (1)$$

Where E_g, h, c and λ are the energy band gap (eV), Planck's constant, the light velocity (m/s) and the wavelength (nm), respectively. DRS results show the effect of transition metals on band structure and energy band gap. UV light absorption for TiO_2 appears at 372 nm in DRS spectra. This absorption is associated with the charge-transfer from oxygen to titanium whose electrons are excited and transferred from the valence band to the conduction band. The observable shifts of the absorbance edge to the visible light region are detected for modified TiO_2 (Table 3). These results show that small amounts of the dopants might be incorporated into the lattice of TiO_2. When transition metal ions are incorporated into the lattice, levels of dopants appear between the valence band and the conduction band, the energy band gap alters and the absorbance edge shifts to the visible light region.

3.2. Kinetic investigation and the mechanism of photocatalytic oxidation

In the photocatalytic process, the efficiency of photooxidation of DMMP at different sampling times is calculated from the Eq. (2).

$$Efficiency\ (\%) = [(C_0 - C)/C_0] \times 100 \quad (2)$$

Here, C_0 is the initial solution concentration and C is the solution concentration after the reaction time. The photocatalytic oxidation of DMMP follows the first-order decay kinetic. Previous studies show that photocatalytic oxidation rate of the most organic compounds, which are in heterogeneous photocatalytic oxidation systems and under UV-light illumination, obey the Langmuir-Hinshelwood (L-H) kinetics model [1,18,19].

Table 3. The results of DRS analysis of photocatalysts.

	TiO_2	Ni/TiO_2	Pd/TiO_2	Pt/TiO_2
λ (nm)	372	387	403	558
E_g (eV)	3.3	3.2	3.0	2.2

$$r = dc/dt = kKC/(1 + KC) \quad (3)$$

In this equation r, C, t, k and K are oxidation rate (mol L^{-1} min^{-1}), concentration of the reactant (mol L^{-1}), illumination time (min), reaction rate constant (min^{-1}) and adsorption coefficient of the reactant (L mol^{-1}) respectively. For low initial DMMP concentrations (when C_0 is small), the rate is proportional to the substrate concentration. In this case, the rate constant is observed to be the pseudo-first order [1]. Therefore, the Eq. (3) can be changed to Eq. (4).

$$Ln(C/C_0) = kKt = k_{app}t \quad (4)$$

Fig. 4 shows the linear behavior of the values calculated from Eq. (4) for palladium containing the catalyst with R^2 = 0.969, which confirms the pseudo-first order reaction. In addition, the apparent rate constant can be calculated from the slope. According to the results, the following mechanism for the oxidation of DMMP on the surface of photocatalyst can be proposed [1,3,9]. Absorbed photons by photocatalysts causes the generation of electron-hole pairs which initiate the photodegradation process. These agents are able to produce superactive radicals like hydroxide ones which attack the organic compounds in the medium and destroy them (Fig. 5). As a result, whatever can delay the electron hole recombination, enhances the concentration of the radicals and the photocatalytic efficiency.

$$TiO_2 + hv \rightarrow TiO_2\ (e^-_{CB} + h^+_{VB}) \quad 1$$
$$TiO_2(h^+_{VB}) + H_2O \rightarrow TiO_2 + H^+ + OH\cdot \quad 2$$
$$TiO_2(h^+_{VB}) + OH^- \rightarrow TiO_2 + OH\cdot \quad 3$$
$$TiO_2(e^-_{CB}) + O_2 \rightarrow TiO_2 + O_2^-\cdot \quad 4$$
$$O_2^-\cdot + H^+ \rightarrow HO_2 \quad 5$$
$$DMMP + All\ radicals \rightarrow Degradation \quad 6$$
$$DMMP + h^+_{VB} \rightarrow Oxidation \quad 7$$

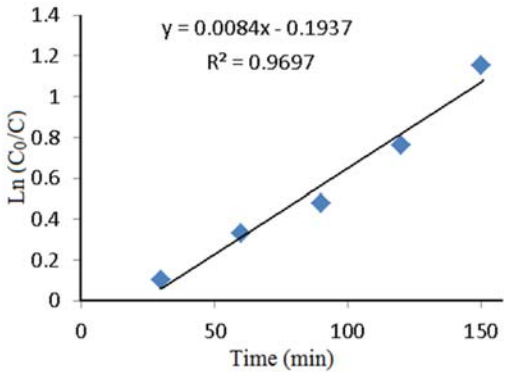

Fig. 4. The photodegradation of DMMP with 1% Pd/TiO_2 after treatment time.

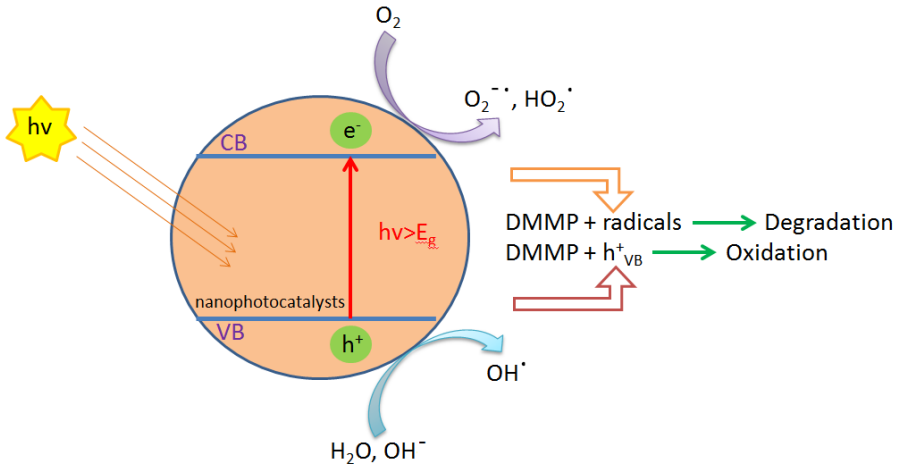

Fig. 5. Mechanism of photocatalytic action of TiO_2 nanocatalysts under UV light irradiation.

3.3. The mechanism of transition metal effect on TiO2 photocatalytic activity

The effect of the type (Pt, Pd and Ni) and amount (0.5, 1.0 and 1.5%) of loading transition metals on the photocatalytic efficiency are shown in Fig. 6 and 7. As can be seen in these figures, the best photooxidation of DMMP was obtained with 1% Pd/TiO_2.

Modified TiO_2 photocatalysts have a higher photoactivity than pure TiO_2. Adding transition metals to the TiO_2 surface can enhance the efficiency of photocatalytic oxidation. Because, the modified TiO_2 particles have a lower crystal size, higher surface area, higher efficiency for the electron-hole regeneration, and higher charge trapping. The charge trapping can be demonstrated by the following equations [1,33].

$$Ti^{4+} + e_{CB}^{-} \rightarrow Ti^{3+} \quad (8)$$

$$M^{n+} + e_{CB}^{-} \rightarrow M^{(n-1)+} \quad (9)$$

$$M^{n+} + h_{VB}^{+} \rightarrow M^{(n+1)+} \quad (10)$$

$$O_2 \text{ or } OH^{-} + h_{VB}^{+} \rightarrow Oxidant\ radicals \quad (11)$$

The holes can transfer to the surface of TiO_2 and react with species in solution (O_2 or hydroxide) to produce the oxidant radicals. When Ti ions of TiO_2 are replaced by transition metal ions, the most of dopant levels appear between the valence band and the conduction band, which can increase the rate of surface trapping of carrier and retard the electron-hole recombination. Therefore, the efficiency of photocatalytic oxidation is enhanced.

3.4. The effect of catalyst dosage

The effect of the photocatalyst dosage on the photooxidation of DMMP solution was studied and the results are presented in Fig. 8. The photocatalytic activities can be related to the availability of active sites on the photocatalyst surface [33]. For 1% Pd/TiO_2, the photo oxidation efficiency is enhanced up to 20 g L^{-1} of the catalyst dosage and then it decreases. The addition of an extra amount of photocatalyst can increase the amount of DMMP absorbed and the number of active catalytic sites for its degradation.

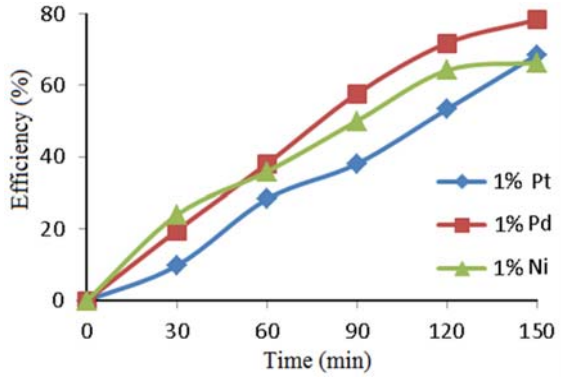

Fig. 6. The effect of type of the loaded metal on the photocatalytic efficiency (DMMP: 0.092 M, catalyst dosage: 10 g L^{-1}, temperature: RT).

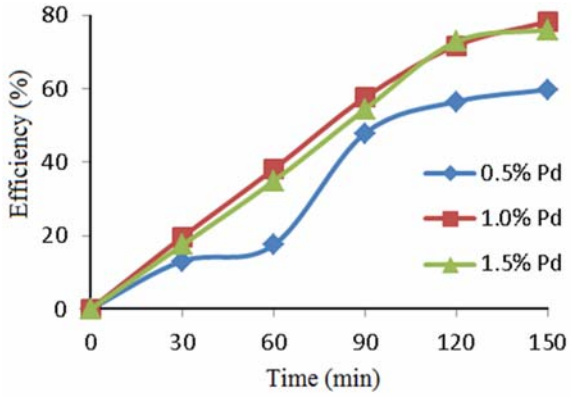

Fig. 7. The effect of the amount of loading metal on the photocatalytic efficiency (DMMP: 0.092 M, catalyst dosage: 10 g L^{-1}, temperature: RT).

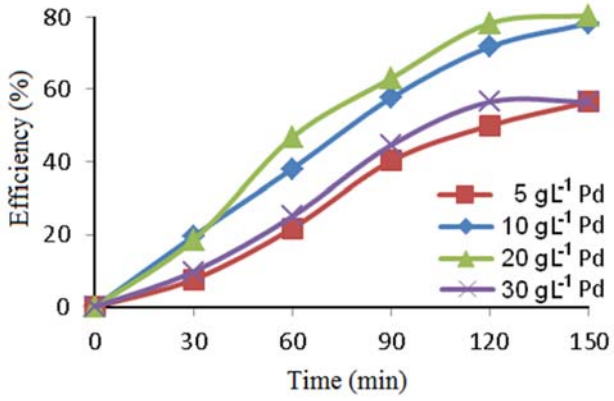

Fig. 8. The effect of catalyst dosage on the photocatalytic oxidation of DMMP (DMMP: 0.092 M, temperature: RT).

However, if the catalyst concentration reaches a specific value, the photooxidation efficiency decreases for different reasons such as agglomeration, light-scattering, and sedimentation of catalyst particles [1,8].

3.5. The effect of initial concentration of DMMP

The effect of the initial DMMP concentration on the photooxidation rate and efficiency is shown in Fig. 9. It was observed that the photooxidation efficiency increases with an increase in the initial concentration of DMMP until 0.138 M at first, and then it decreases. This may be attributed to the fact that the active sites of the catalyst are covered by the organic compound present at high concentration and, therefore, a significant amount of UV light may be absorbed by the organic molecules rather than by the catalyst particles [26]. Thus, the generation of oxidant radicals on the surface of catalysts is reduced and the efficiency of DMMP photooxidation is decreased.

4. Conclusion

TiO_2 based photocatalysts modified with transition metals Pt, Pd and Ni were synthesized by sol-gel method. The prepared photocatalysts were characterized by different analysis methods such as XRD, FTIR, SEM, DRS and BET. The photocatalytic properties of the prepared samples were evaluated by photooxidation of DMMP as an organophosphorus simulant of chemical warfare agent. A kinetic and mechanistic study was performed and the photocatalytic oxidation of DMMP with palladium containing the catalyst followed the pseudo first-order decay kinetic. The effects of some parameters such as photocatalyst dosage, initial concentration of DMMP and the amount and type of loading impurities on the photocatalytic efficiency were studied. The results showed that the best photoactivity was obtained with

1% Pd/TiO_2. According to the results, at first, the photooxidation efficiency increased with an increase in the catalyst dosage and initial concentration of DMMP and then it decreased.

References

[1] S. Ghasemi, S. Rahimnejad, S. Rahman Setayesh, S. Rohani, M.R. Golami, J. Hazard. Mater. 172 (2009) 1573-1578.
[2] R.J. Tayade, R.G. Kulkarni, R.V. Jasro, Ind. Eng. Chem. Res. 45 (2006) 5231-5238.
[3] C. Dominguez, J. Garcia, M.A. Pedraz, A.A. Torres, M.A. Galan, Catal. Today 40 (1998) 85-101.
[4] M.H. Habibi, E. Askari, Iran. J. Catal 1 (2011) 41-44.
[5] H. Faghihian, A. Bahranifard, Iran. J. Catal 1 (2011) 45-50.
[6] H.R. Pouretedal, S. Basati, Iran. J. Catal. 2 (2012) 51-55.

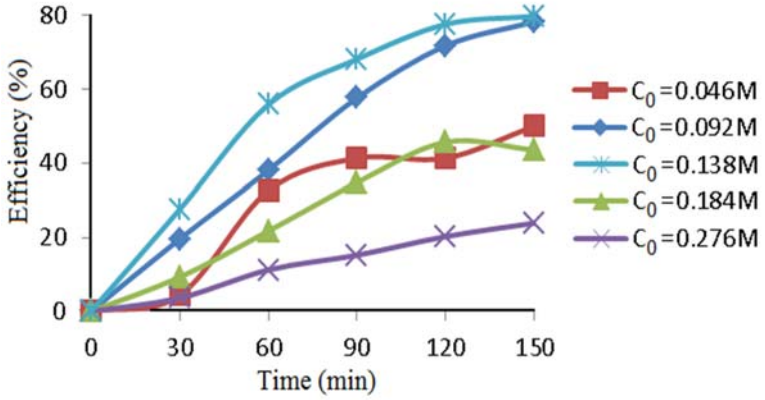

Fig. 9. The effect of initial DMMP concentration on the photocatalytic oxidation of DMMP (catalyst dosage: 10 g L^{-1}, temperature: RT).

[7] H.R. Pouretedal, M. Ahmadi, Iran. J. Catal. 3 (2013) 149-155.
[8] S. Malato, J. Blanco, A.R. Fernández-Alba, A. Agüera, Chemosphere 40 (2000) 403-409.
[9] J.P. Percherancier, R. Chapelon, B. Pouyet, J. Photochem. Photobiol. A 87 (1995) 261-266.
[10] R.A. Doong, W.H. Chang, J. Photochem. Photobiol. A 107 (1997) 239-244.
[11] M. Kerzhentsev, C. Guillard, J.M. Herrmann, P. Pichat, Catal. Today 27 (1996) 215-220.
[12] M. Arami, N. Yousefi Limaee, N.M. Mahmoodi, N. Salman Tabrizi, J. Hazard. Mater. 135 (2006) 171-179.
[13] S. Gautam, S.P. Kamble, S.B. Sawant, V.G. Pangarkar, Chem. Eng. J. 110 (2005) 129-137.
[14] S Malato, J Blanco, M.I. Maldonado, P. Fernandez-Ibanez, A. Campos, Appl. Catal. B 28 (2000) 163-174.
[15] A.L. Linsebigler, G. Lu, J.T. Yates, Chem. Rev. 95 (1995) 735-758.
[16] M. Kaneko, I. Okura, Photocatalysis, Science and Technology, Springer, Germany, 2002.
[17] A. Hagfeldt, M. Graetzel, Chem. Rev. 95 (1995) 49-68.
[18] P.V. Kamat, Chem. Rev. 93 (1993) 267-300.
[19] N. Serpone, E. Pelizzetti, Photocatalysis: Fundamentals and Application", John Wiley & Sons, New York, 1989.
[20] A. Mills, S. Le Hunts, J. Photochem. Photobiol. A 108 (1997) 1-35.
[21] M.A. Fox, M.T. Dulay, Chem. Rev. 93 (1993) 341-357.
[22] W.Y. Ching, J. Am. Ceram. Soc. 73 (1990) 3135-3159.
[23] M.S. Ahmed, Y.A. Attia, J. Non-Cryst. Solids 186 (1995) 402-407.
[24] G. Balasubramanian, D.D. Dionysiou, M.T. Suidan, Dekker Encyclopedia of Nanoscience and Nanotechnology, Vol. 6, Marcel Dekker Inc., New York, 2004.
[25] J. Hagen, Industrial Catalysis: A Practical Approach, 2nd Ed., John Wiley & Sons, Germany, 2006.
[26] I.K. Komstantinou, T.A. Albanis, Appl. Catal. B 49 (2004) 1-14.
[27] Y. Ishibai, J. Sato, T. Nishikawa, S. Miyagishi, Appl. Catal. B 79 (2008) 117-121.
[28] J.M. Kwon, Y.H. Kim, B.K. Song, S.H. Yeom, B.S. Kim, J.B. Im, J. Hazard. Mater. 134 (2006) 230-236.
[29] E. Bizani, K. Fytianos, I. Poulios, V. Tsiridis, J. Hazard. Mater. 136 (2006) 85-94.
[30] S.L. Bartelt-Hunt, D.R.U. Knappe, M.A. Barlaz, Crit. Rev. Env. Sci. Tech. 38 (2008) 112-136.
[31] A. Besharati-Seidani, M.R. Gholami, Iran. Chem. Chem. Eng. J. 34-1 (2015) 39-49.
[32] M. Padervand, M. Tasviri, M.R. Gholami, Chem. Papers 65 (2011) 280-288.
[33] M.N. Rashed, A.A. El-Amin, Int. J. Phys. Sci. 2 (2007) 73-81.